

UNLIMITED DISTRIBUTION



National Defence  
Research and  
Development Branch

Défense Nationale  
Bureau de Recherche  
et Développement

TECHNICAL MEMORANDUM 86/206

January 1986

UNLIMITED  
DISTRIBUTION  
ILLIMITÉE

SOME WARSHIP SLAMMING  
INVESTIGATIONS

W.C.E. Nethercote  
M. MacKay - B. Menon

Defence  
Research  
Establishment  
Atlantic



Centre de  
Recherches pour la  
Défense  
Atlantique

Canada

**DEFENCE RESEARCH ESTABLISHMENT ATLANTIC**

9 GROVE STREET

P.O. BOX 1012  
DARTMOUTH, N.S.  
B2Y 3Z7

TELEPHONE  
(902) 426-3100

**CENTRE DE RECHERCHES POUR LA DÉFENSE ATLANTIQUE**

9 GROVE STREET

C.P. 1012  
DARTMOUTH, N.É.  
B2Y 3Z7

UNLIMITED DISTRIBUTION



National Defence  
Research and  
Development Branch

Défense Nationale  
Bureau de Recherche  
et Développement

SOME WARSHIP SLAMMING  
INVESTIGATIONS

W.C.E. Nethercote  
M. MacKay - B. Menon\*

January 1986

Approved by T. Garrett Director/Technology Division

DISTRIBUTION APPROVED BY

D/TD

TECHNICAL MEMORANDUM 86/206

Defence  
Research  
Establishment  
Atlantic



Centre de  
Recherches pour la  
Défense  
Atlantique

Canada

\*ARCTEC CANADA LTD.

## ABSTRACT

Excessive slamming is the most common cause of speed reduction for frigates and destroyers in heavy head seas. DREA's early interest in frigate/destroyer slamming was limited to the development of computer programs for ship seakeeping performance prediction. Published bottom slamming algorithms were adopted and refined to provide a slamming prediction capability for DREA software. In follow-on work described herein, both two-dimensional numerical simulations and three-dimensional model tests were performed by contractors to obtain better physical insight and expand the empirical data base. The two-dimensional numerical simulation results required considerable smoothing to reduce numerical noise, but still yielded form factors in satisfactory agreement with two-dimensional theoretical and experimental results. The simulations also gave unique insight into the girthwise development of slamming pressures. The three-dimensional model tests indicated that pivoted drop tests in waves may be substituted for conventional seakeeping tests, but the general applicability of the results was limited by difficulties with measurement of relative impact velocity. Notwithstanding the velocity measurement difficulties, the three-dimensional tests provided important information on longitudinal and girthwise pressure pulse velocities. Further experimental work will be required to develop a usable experimental data base.

## RÉSUMÉ

Un tapement excessif est la cause la plus commune de la réduction de vitesse des frégates et destroyers par fortes mers debout. Les premières recherches du CRDA sur le tapement des frégates et destroyers se limitaient à la mise au point de programmes d'ordinateur pour la prévision du rendement des navires en termes de tenue à la mer. Des algorithmes publiés de tapement ont été adoptés et raffinés de manière à permettre la prévision du tapement au moyen du logiciel du CRDA. Lors des travaux complémentaires décrits, des simulations numériques bidimensionnelles et des essais tridimensionnels sur modèles ont été effectués par des entrepreneurs afin d'éclairer l'aspect physique et d'étendre la base de données empiriques. Un lissage considérable des résultats de simulation numérique bidimensionnelle était nécessaire afin de réduire le bruit numérique, mais on a tout de même obtenu des facteurs de forme concordant d'une manière satisfaisante avec les résultats bidimensionnels théoriques et expérimentaux. Les simulations ont de plus fourni un aperçu inégalé de la propagation des pressions de tapement suivant le périmètre. Les essais tridimensionnels sur modèles ont également indiqué que l'on pouvait substituer des essais de chute avec pivotement dans les vagues aux essais classiques de tenue à la mer, mais que l'applicabilité générale des résultats était limitée par des difficultés de mesure de la vitesse relative d'impact. Malgré ces difficultés de mesure de la vitesse, les essais tridimensionnels ont fourni des renseignements importants sur les vitesses longitudinale et suivant le périmètre de l'impulsion de pression. D'autres travaux expérimentaux seront nécessaires pour l'obtention d'une base de données expérimentales utilisable.

## TABLE OF CONTENTS

ABSTRACT	ii
TABLE OF CONTENTS	iv
NOTATION	v
1. INTRODUCTION	1
2. DREA'S BACKGROUND WORK	1
2.1 Early Slamming Algorithms	2
2.2 Improved Slamming Algorithms	3
3. IDENTIFICATION OF REQUIRED WORK	6
4. COMPUTER SIMULATIONS	7
4.1 Background	7
4.2 Test Cases	8
4.3 Numerical Model	8
4.4 Discretisation Noise	9
4.5 Surge and Section Dynamics	10
4.6 Impact Pressure Distribution	12
4.7 Form Factor	13
5. EXPERIMENTAL WORK	16
5.1 Drop Test Programme	16
5.2 Seakeeping Test Programme	18
5.3 Results	21
5.3.1 Drop Tests	21
5.3.2 Seakeeping Tests	26
6. SIMULATION/MODEL TEST COMPARISONS	27
7. CONCLUDING REMARKS	30
8. ACKNOWLEDGEMENTS	31
REFERENCES	33

## NOTATION

A, B, C, K	subscripts for pressure transducer locations
$\bar{c}$	assumed speed of sound in water
h	half-siding
h	time, hours
k	form factor
k'	corrected form factor, per equation 12
l	grid dimension for numerical simulation
L	length between perpendiculars
p	impact pressure
P <sub>h</sub>	most probable extreme pressure in h hours
P <sub>MAX</sub>	maximum slamming pressure
P <sub>t</sub>	most probable impact pressure in t seconds
P(...)	probability of occurrence
s	girth
t	time, seconds
T	draft
$\hat{v}$	threshold velocity
V	vertical ship/section velocity
V <sub>h</sub>	horizontal component of wave velocity
V <sub>o</sub>	initial impact velocity
V <sub>on</sub>	velocity component normal to wave
V <sub>ot</sub>	velocity component tangential to wave
V <sub>v</sub>	vertical component of wave velocity
x	undisturbed waterline corresponding to y
$\bar{x}$	x corrected for surge

X, Y, Z	hull coordinate system
y	penetration
$\alpha$	buttock angle
$\alpha$	parameter for extreme pressure probability, Figure 4
$\beta$	deadrise angle
$\theta$	wave slope
$\mu$	surge ratio
$\lambda$	wave length
$\zeta_A$	wave amplitude
$\xi, \eta$	body-fixed coordinates, Figure 8
$\rho$	density of water
$\sigma_{RM}$	RMS relative motion
$\sigma_{RV}$	RMS relative velocity
$\tau$	pitch angle

Note: The symbols  $h$  and  $\alpha$  both represent two parameters, but in each case the symbol is in conventional use, so the duplication was retained. The appropriate definition is made clear in the context of each application.



1.        **INTRODUCTION**

For warships of frigate/destroyer size, excessive slamming is the most common reason for speed reduction in heavy seas; thus, a principal goal in hull form research and development is the improvement of slamming characteristics. An implicit requirement for such improvement is the development of accurate slamming prediction capabilities.

DREA's early interest in slamming was linked to the development of computer programs for ship seakeeping performance prediction. These programs, of the common frequency domain, linear strip-theory type, adapted existing methods to provide predictions of bottom slam pressures and total slam force.

Notwithstanding development of these prediction capabilities, it was recognized that there was still a requirement for more fundamental information on bottom slamming, so further work was conducted, both analytical and experimental. In the first instance, the commercially available computer code PISCES 2DELK was used to simulate drop tests of 2-D wedges, truncated wedges and ship sections. In the second approach, ARCTEC Canada Limited were contracted to conduct an experimental program.

The computer simulations provided time histories of local pressures, total force and section dynamics, as well as the development of the girthwise pressure time history. After smoothing to reduce numerical noise, the data were used to derive form factors, which satisfactorily agreed with two-dimensional experimental results.

The experimental work was directed towards development of a data base containing slam-related quantities for warship hull forms. Three warship hull forms, with 'U', 'normal' and 'V' bow sections were used in vertical and pivoted drops, in waves as well as in still water. Seakeeping tests were also carried out with the V bow form. Measurements included local peak pressure, pressure rise time, pulse duration and frequency, for up to 24 transducers.

This memorandum describes the above work and summarizes earlier slamming research at DREA. The two-dimensional simulations have provided insight into the fundamental details of the process, but it is clear that three-dimensional model data are essential to the achievement of realistic ship slam pressure predictions. Experimental techniques must be refined before a useful data base can be created.

2.        **DREA'S BACKGROUND WORK**

The catalyst for slamming research at DREA was the development of an in-house computer program for predicting ship motions. PHHS<sup>1</sup> (Pitch

and Heave in Head Seas) employed conventional strip theory for the calculation of vertical plane motions in unidirectional head seas. This coding was subsequently used together with methodology proposed by Salvesen, Tuck and Faltinsen<sup>2</sup> and enhanced by Schmitke<sup>3</sup> to develop a 6 degree-of-freedom prediction capability.

The utility of PHHS was greatly increased by the addition of algorithms for added resistance, relative motion corrections (wave profile and dynamic swell-up), deck wetness, slamming pressures and human tolerance to vertical motion. Some of these capabilities were unique among contemporary computer programs. Relative motion corrections were of particular importance in rectifying strip theory's typically poor prediction of deck wetness; for example, see Schmitke's contribution to the discussion of Reference 4.

## 2.1 Early Slamming Algorithms

The first slamming calculations were based on the statistical theory of Ochi and Motter<sup>5</sup> together with Chuang's<sup>6</sup> experimental impact data. In the conventional manner, slamming was taken to be dependent upon keel emergence and the reaching of a threshold relative velocity on impact. The probability of keel emergence is:

$$P(\text{keel emergence}) = P(\text{keel}) = \exp [-T^2 / 2\sigma_{RM}^2] \quad (1)$$

where  $T$  is draft and  $\sigma_{RM}$  is root mean square relative motion, corrected for dynamic swell-up. Slam probability is then

$$P(\text{slam}) = \exp [-\hat{v}^2 / 2\sigma_{RV}^2] P(\text{keel}) \quad (2)$$

where  $\sigma_{RV}$  is RMS relative velocity and the slamming threshold velocity,  $v$ , is given by

$$v = 0.0195 \sqrt{gL} / (0.03 \cot \beta + h/B) / 2 \quad (3)$$

where  $L$  is the LBP,  $\beta$  is local deadrise angle,  $h$  half-siding and  $B$  beam.

The probability of slamming is of rather academic interest compared to the consequent slamming pressures. As per Ochi and Motter, PHHS calculated the most probable peak impact pressure in  $t$  seconds:

$$P_t = \rho k \sigma_{RV}^2 \ln \{ t \sigma_{RV} / 2\pi \sigma_{RM} P(\text{keel}) \} \quad (4)$$

The section form factor,  $k$ , was obtained from a statistical fit to Chuang's data as shown in Figure 1:

$$k = 1 + (1 - \exp(-5 \beta)) (\pi/2 \cot \beta)^2 \quad (5)$$

The above expression is a reasonably good model of the experimental data for  $\beta > 5^\circ$ .

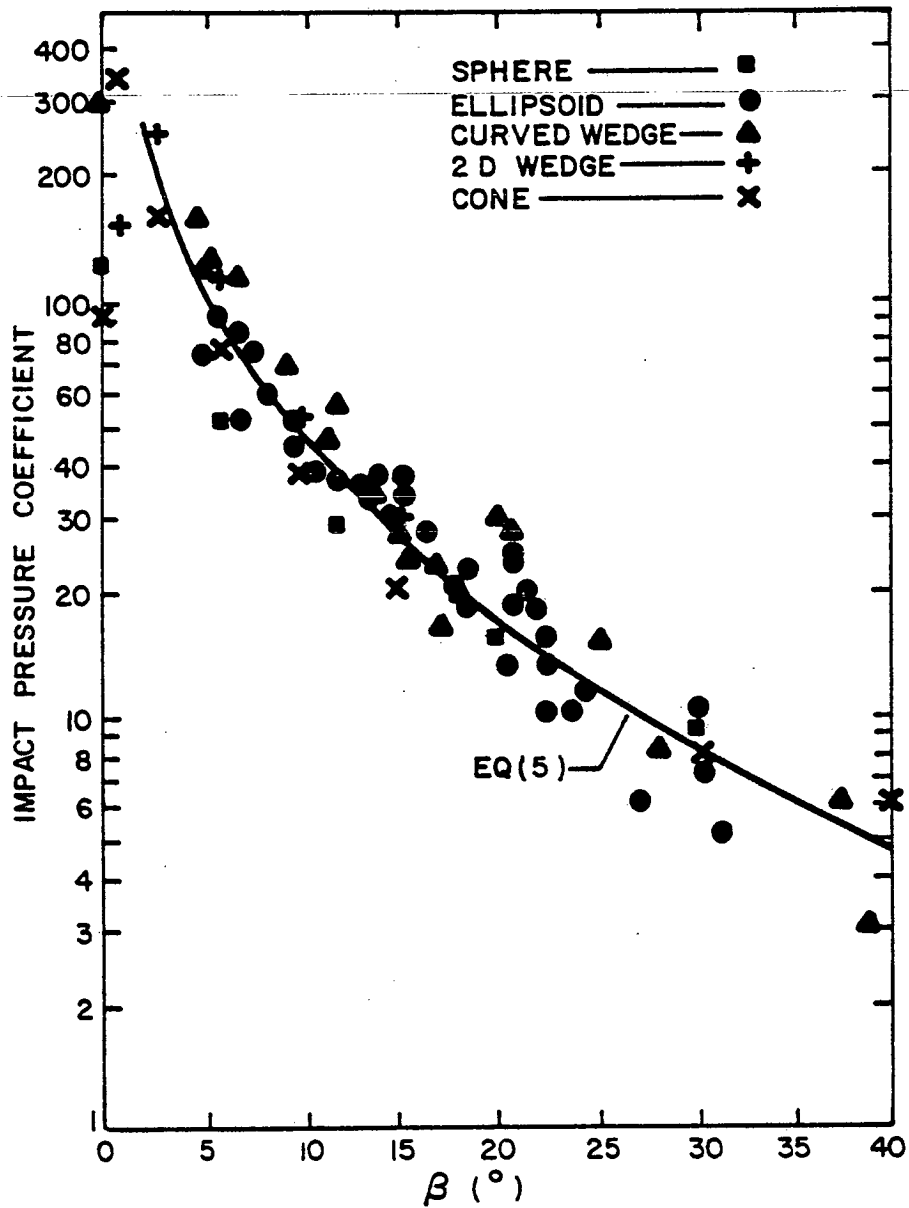


Figure 1 Chuang's Impact Pressure Coefficient

## 2.2 Improved Slamming Algorithms

The early slamming algorithms were open to question through their use of prism impact data, as suggested by comparative work by Ochi and Bonilla-Norat<sup>7</sup> and Schenzle et al<sup>8</sup>. The reply to discussion of Reference 5 dealt with the large magnitude of 2-D section impact pressure

coefficients, or form factors, at some length. Order of magnitude differences between drop and seakeeping test derived form factors were often observed, especially at low deadrise angles.

From analysis of model and full-scale seakeeping data, Ochi and Motter chose a threshold velocity of 12 ft/sec for a 520 ft ship. Through Froude scaling this generalised to

$$\hat{v} = 0.0927 (gL)^{1/2} \quad (6)$$

This expression may be criticised for its independence of section shape. Schmitke<sup>9</sup> proposed an alternative derived from Ochi's work:

$$\hat{v} = 0.377 (gL/k)^{1/2} \quad (7)$$

which was obtained by multiplying equation (6) by  $(16.56/k)^{1/2}$ ; 16.56 is the k value for Station 3 of Ochi's Mariner hull-form, used in the derivation of equation (6). In this way, a threshold impact pressure can be defined:

$$p \geq (\rho/2)k \hat{v}^2 = 0.0711\rho gL \quad (8)$$

Schmitke noted that equations (7) and (3) produce comparable results for V-bowed warships.

In modifying the algorithms, the very apparent conservatism of prism impact data was recognized and the Ochi-Motter predictor based on experiments with Mariner models<sup>10</sup> was adopted for cases with known section offsets. A simplified option allowing the specification of deadrise angle only was also developed using the routines of Reference 10 to generate form factors for a series of truncated wedges (Figure 2) where

$$5^\circ \leq \beta \leq 20^\circ$$

$$T = 15 \text{ ft}$$

$$h = 0.5 \text{ ft.}$$

For  $\beta$  less than 5 degrees, k was taken as 30. Since at  $\beta$  of 21 degrees the Ochi-Motter and Stavovy-Chuang<sup>11</sup> methods produced similar results, the results of the two methods were coupled together as shown in Figure 3. Further reference will be made to this combination later.

Slamming probability is of little value itself, so the Ochi-Motter method was again used to calculate the most probable extreme pressure in h hours of operation:

$$P_h = \rho k \sigma^2_{RV} \ln[3600P(\text{keel})h \sigma_{RV}/(2\pi\sigma_{RM})] \quad (9)$$

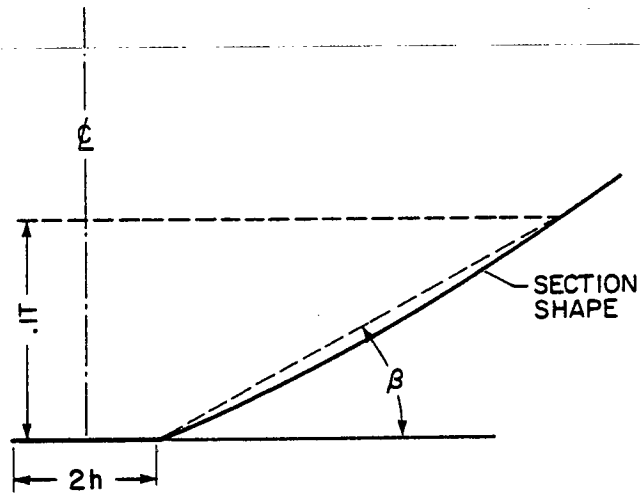


Figure 2 Truncated Wedge Approximation

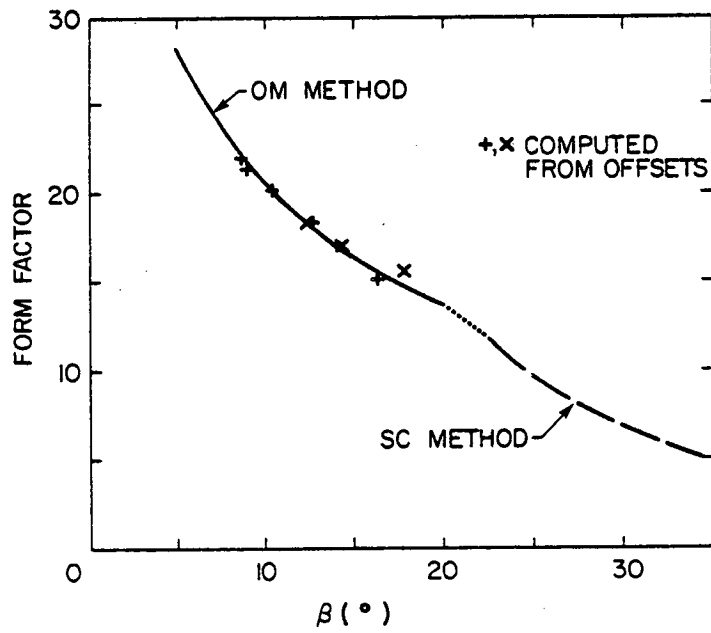


Figure 3 Form Factor For Truncated Wedges

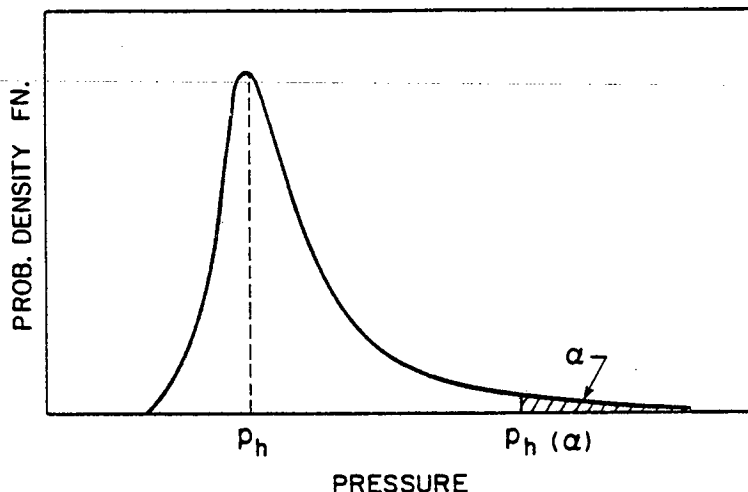


Figure 4 Slamming Pressure Probability Density Function

Figure 4 shows that the probability of exceeding  $p_h$  is too high to be an acceptable design value, so an extreme pressure is calculated:

$$p_h(\alpha) = \rho k \sigma^2_{RV} \ln[3600P(\text{keel})h \sigma_{RV} / (2\pi\alpha \sigma_{RM})] \quad (10)$$

where  $p_h(\alpha)$  is the extreme pressure whose probability of being exceeded in  $h$  hours is  $\alpha$ . Note that both  $p_h$  and  $p_h(\alpha)$  are independent of  $V$ . Reference 4 regards 0.01 as a reasonable value for  $\alpha$ .

### 3. IDENTIFICATION OF REQUIRED WORK

A number of points became apparent in evaluating the literature, the most important being:

- that seakeeping and drop tests predict inconsistent slam pressures;
- that full-scale and model-scale seakeeping tests yield consistent slam pressures; and,
- that the available seakeeping-based algorithms are derived from limited data, the bulk of which is representative of merchant ship rather than warship design practice.

In view of these deficiencies ARCTEC Canada Ltd. was contracted to carry out a comprehensive series of experiments at model scale including three-dimensional drop tests and seakeeping tests. The contract called for:

- a state of the art survey of experimental methods in slamming;
- an evaluation of current capabilities of experimental facilities;
- an experimental program to acquire slamming data for warship hulls; and
- development of a preliminary semi-empirical prediction method.

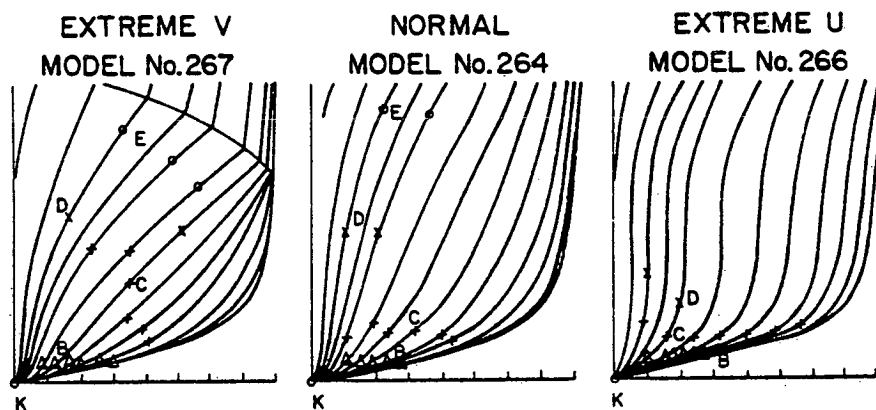


Figure 5 Pressure Transducer Locations on Bow Forms

The experimental program made use of hull forms developed by the National Research Council of Canada's Institute of Marine Dynamics (IMD) for a fast surface ship methodical series.<sup>1,2</sup> Normal, extreme-V and extreme-U designs shown in Figure 5 were selected for experiments.

In parallel with the experimental work, numerical simulations were performed to examine some of the fundamental features of ship slamming.

#### 4. COMPUTER SIMULATIONS

##### 4.1 Background

In order to gain a greater insight into the physical parameters affecting the slamming process, a series of computer simulation cases was run. Computer code PISCES 2DELK (a trademark of Physics International Company, California) was selected for the work. It is available in Canada on the CDC CYBERNET system. Individual cases were set up and run by CDC CYBERNET. The resulting data were transferred to DREA for reduction and analysis.

PISCES 2 DELK is a two-dimensional finite difference code with Eulerian, Lagrangian and shell-structure capabilities. It was designed to simulate high velocity impacts and explosions, i.e. over time scales shorter by up to several orders of magnitude than those characterising a ship slam. The implications of this to the present work are noted in Section 4.3. The methods employed by PISCES 2DELK are described in detail in Reference 13.

#### 4.2 Test Cases

Each case run differed in geometrical parameters and in initial impact velocity. Three, two-dimensional geometrical forms were tested: simple wedges, wedges truncated at the keel to represent half-siding, and forward sections (here referred to as frigate sections) from the 'normal' model No. 264. For wedges, the geometrical parameter was deadrise angle,  $\beta$ , which could take a value of 10, 20, 30, or 40 degrees. Sections 3, 4, and 5 (0 at FP and 20 at AP) were used from model 264. Full scale impact velocity was 10, 15, 20 or 30 ft/sec.

#### 4.3 Numerical Model

Simulations were run using full scale dimensions. The section fell under the influence of gravity, simulating a free drop test. Figure 6 illustrates the initial (time = zero) geometry for a simple wedge. The water, and a void region above it, were discretised in an Eulerian (fixed) grid. The void allowed upward deformation of the free surface. The

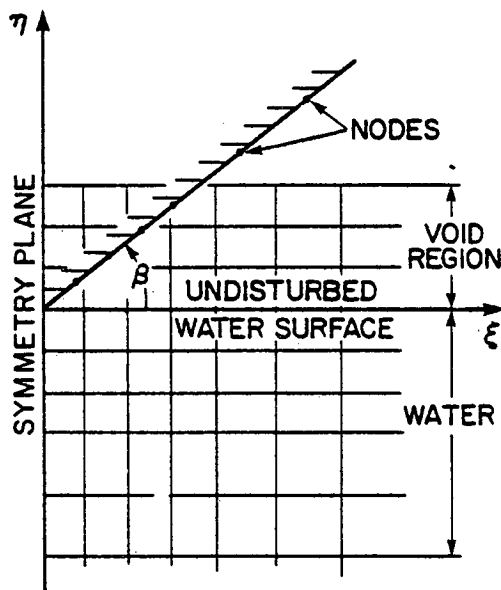


Figure 6 Initial Geometry for Numerical Simulation



impacting section was assumed to be rigid, its boundary defined by a Lagrangian (moving) grid. Standard material properties were modified to ensure section rigidity and to reduce the speed of sound in water, as noted below.

The equations of motion were solved explicitly in time. In order to ensure stability of the solution, the time step  $\Delta t$  was restricted to a fraction of  $\ell/c$ , where  $\ell$  is the minimum cell dimension in the Eulerian grid and  $c$  is the assumed speed of sound in water. To achieve a reasonable value for  $\Delta t$ , given  $\ell$ , the assumed speed of sound was reduced from the true value, with the limitation that the local Mach number nowhere exceed 0.1, so that the effects of compressibility on impact dynamics could be neglected.

#### 4.4 Discretisation Noise

The data were generally quite noisy, as illustrated by Figure 7. Each curve on the figure shows pressure as a function of girth at a time indicated by the right-hand vertical scale. For low deadrise cases the pressure distribution showed strong periodicity, attributed to interaction between the grid systems. The initial spikes on the keel, for all cases with half-siding, were found to be close to the acoustic pressure limit,  $\rho V_0 c$ . The pressure data could be smoothed by repeated local averaging, but this destroyed the peak structure of the distribution.

Total vertical force was smoothed by local averaging of the cumulative impulse a number of times, and then differentiating the result.

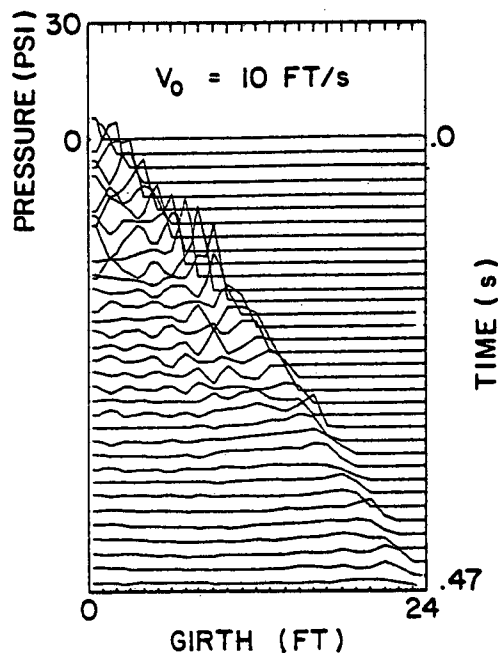


Figure 7 Impact Pressure Distributions for a 20 Degree Truncated Wedged

#### 4.5 Surge and Section Dynamics

The parameters for a simple wedge during impact are shown in Figure 8. Surge is conveniently represented by the ratio  $\mu = \bar{x}/x$ . Since the water surface was free to deform in the simulations, surge could be

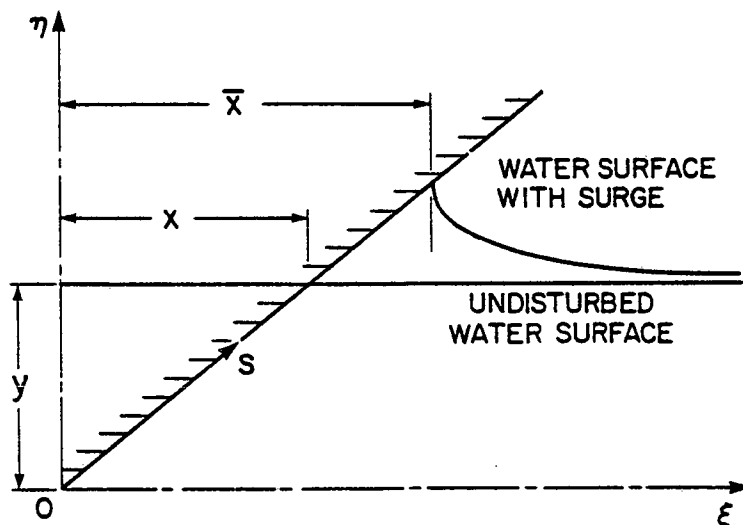


Figure 8 Impact Geometry

readily estimated as illustrated by Figure 9 (the arrows in the figure indicate magnitude and velocity direction in the field). The value of  $\mu$  observed was initially high but rapidly settled to a near constant value. These estimates of  $\mu$  for the wedge cases are compared in Figure 10 with the theoretical approximation of Geers et al<sup>14</sup> and with two theoretical models of Chu and Abramson<sup>15</sup>. Good correlation with the flat plate model can be seen, although selected experimental data cited in Reference 15 are consistently lower than the theoretical models at small deadrise angles.

The surge ratio has some significance for impact force as shown by Figure 11. The curves identified as 'R-K simulation' were obtained by integrating the equations of motion for a wedge using a Runge-Kutta method. Two values of  $\mu$  were used in these calculations: the simulation estimate for this particular case, 1.69; and the average of estimates for all 20 degree wedge simulations, 1.77. The resulting 5 percent increment in surge ratio produces a 5 percent increase in vertical force. The third curve is the result of a PISCES simulation with 50 smoothing iterations applied. Even this amount of smoothing does not eliminate discretisation noise entirely.

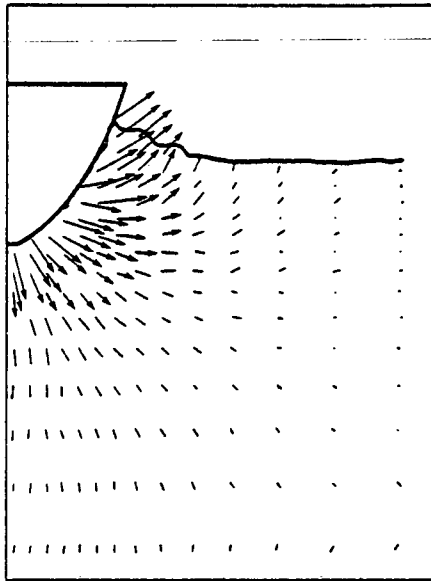


Figure 9 Frigate Section 3 after 0.367 Seconds:  
Initial Velocity 10 FPS

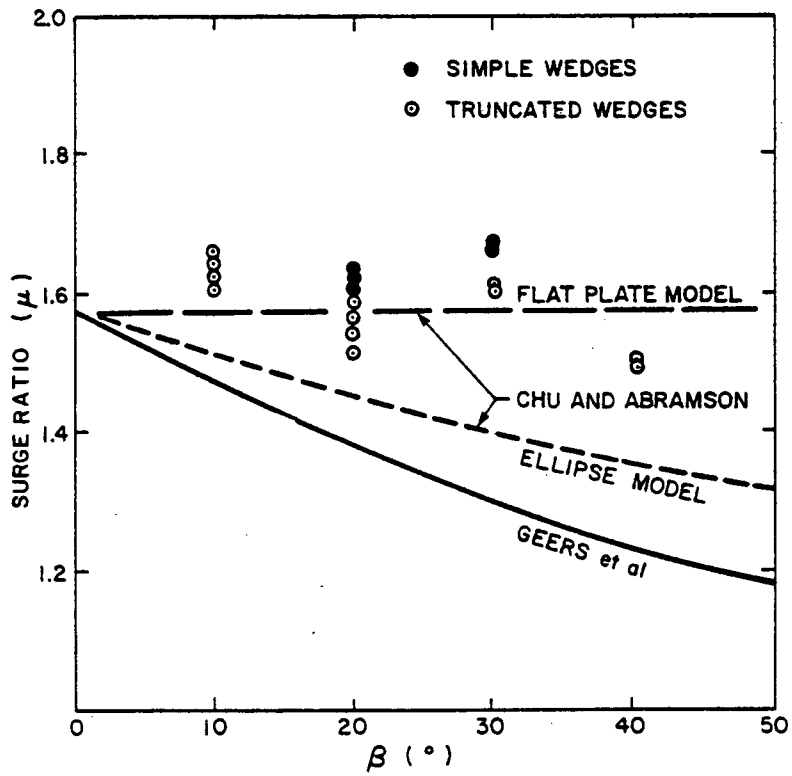


Figure 10 Surge Ratio for Simple and Truncated Wedges

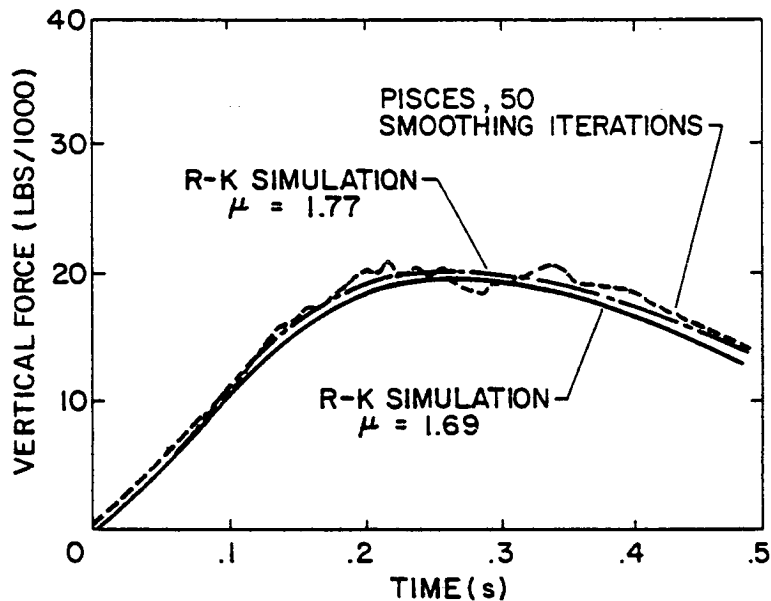


Figure 11 Time Histories of Vertical Force for a 20 Degree Simple Wedge with Initial Velocity 10 FPS

#### 4.6 Impact Pressure Distribution

Although, as previously noted, the discretisation employed in these simulations was too coarse to adequately distinguish sharp peaks, the pressure signatures and the maxima occurring after the initial impact were in general fairly well represented, even after a number of smoothing iterations. To better determine the initial peaks, finer grids and shorter time steps could be used, but at much greater computational cost.

A typical set of pressure distributions for a truncated wedge was presented in Figure 7. Very little difference between simple and truncated wedges was observed. Some difference was seen in the initial peaks but these were heavily contaminated with noise; after a few time steps the distributions were virtually indistinguishable. After initial impact, most wedge cases approximated the classic Wagner<sup>16</sup> pressure distribution, being fairly uniform in the region of the keel, rising to a peak (the amplitude of which depended on smoothing) at the waterline.

Pressure distributions for the frigate sections showed different characteristics as typified by Figure 12. Although initially like the wedge pressure distributions, the keel pressure falls more slowly with time while the waterline peak rapidly disappears. This results in the developed

pressure distribution having a triangular appearance as clearly shown in the figure. The wedges with highest deadrise, 40 degrees, exhibited intermediate behaviour, with the change from a Wagner pressure distribution to triangular being considerably delayed compared with the frigate sections.

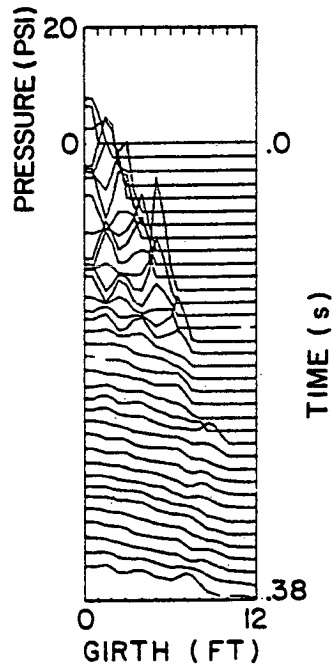


Figure 12 Impact Pressure Distributions for Frigate Section 4

#### 4.7 Form Factor

Because of discretisation noise, the pressure distribution alone would not give a good estimate of form factor,  $k$ , in the basic impact equation:

$$P_{MAX} = (\rho/2)kV^2 \quad (11)$$

A number of alternative methods to evaluate form factor were tried; none were entirely satisfactory for frigate sections. One of the better methods for wedges consisted of obtaining a linear least-squares unbiased estimate of  $k$  from the total vertical force produced by a modified Wagner pressure distribution. If  $k$  is constant, not only should the estimate be asymptotic in time, but also uncertainty is progressively reduced. This was found to be so for most wedge cases, as illustrated by

Figure 13. As shown in the figure, after some initial excursions, the estimate stayed at a plateau for a while before falling slowly in value. This fall coincides with the decay of the Wagner pressure distribution.

Form factor, taken to be the aforementioned plateau value, is plotted versus wedge deadrise in Figure 14. The curves plotted for comparison are: Wagner - the classical result, Drop Tests - equation (5), and SC-OM - Figure 3.

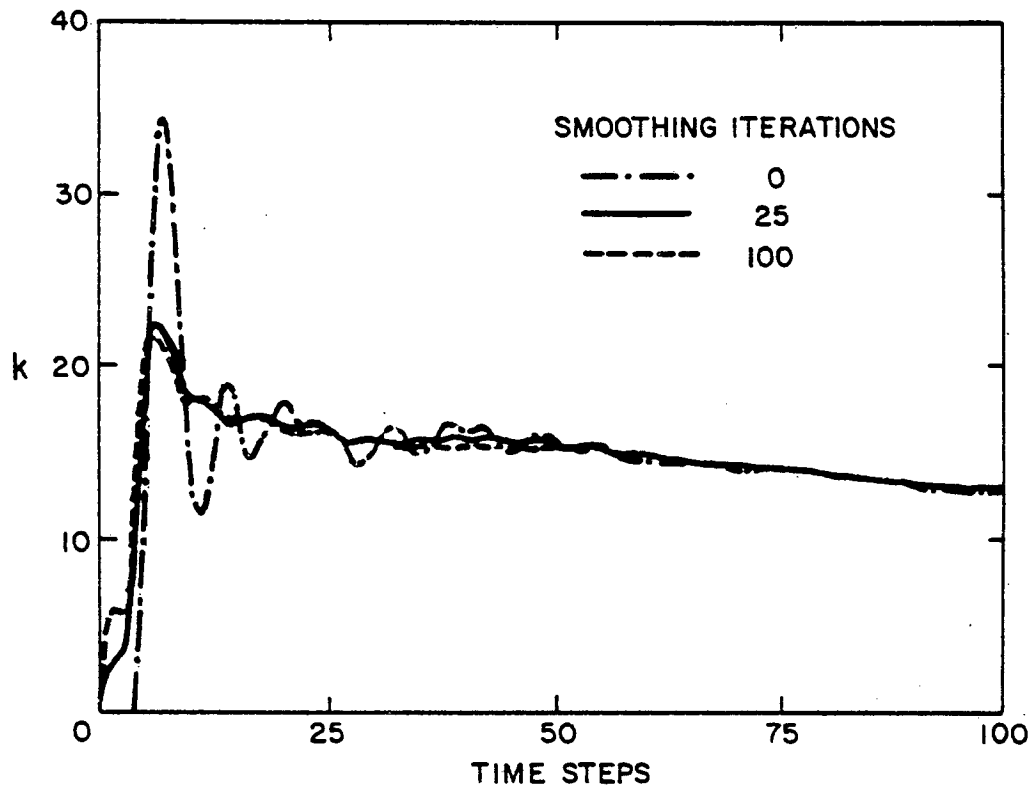


Figure 13 Convergence of Form Factor Estimate for Simple 20 Degree Simple Wedge with Initial Velocity 10 FPS

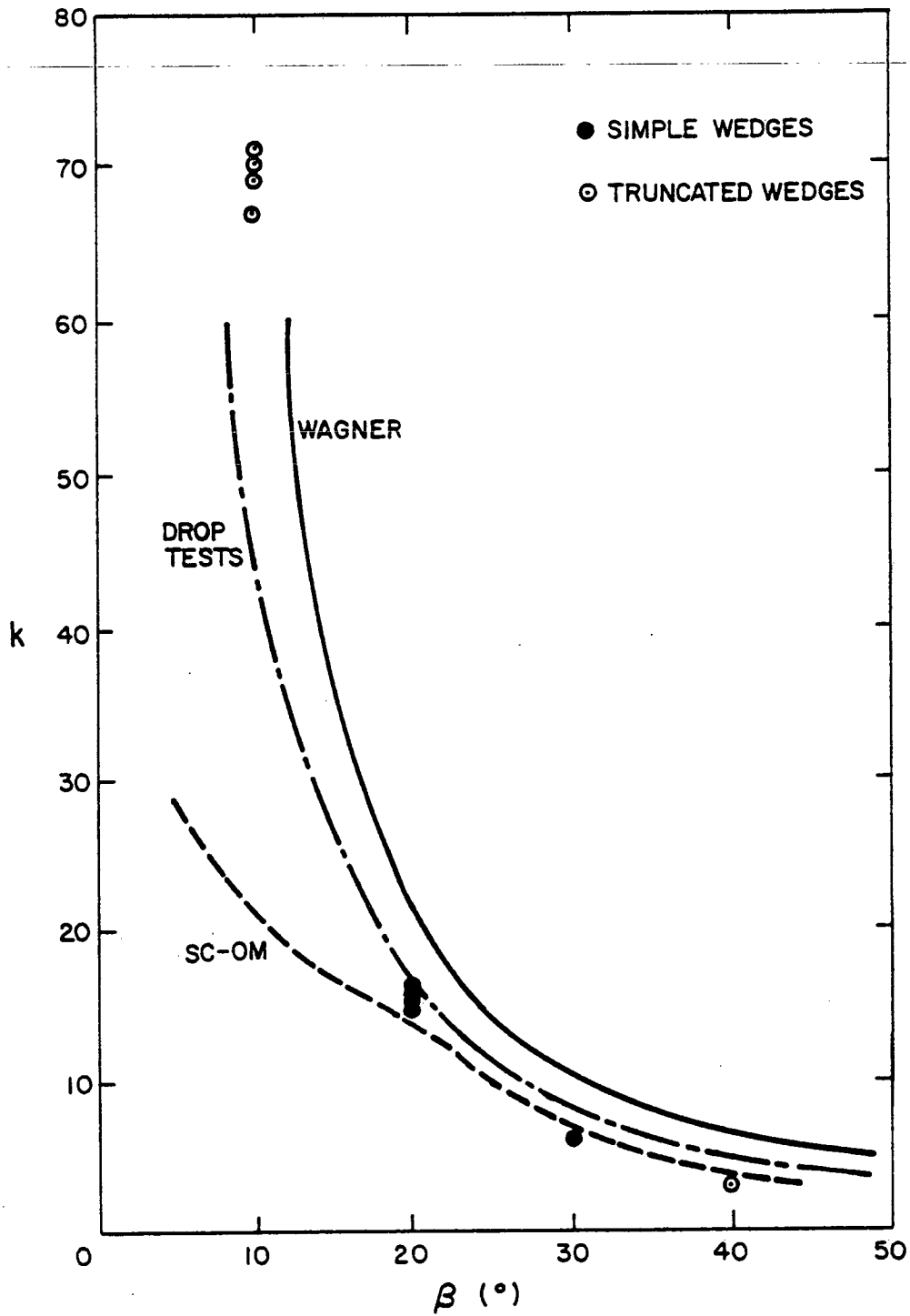


Figure 14 Form Factor for Simple and Truncated Wedges

## 5. EXPERIMENTAL WORK

The experimental program was preceded by an extensive review of the literature. In all published sources, there is serious discrepancy between the results of the various types of slamming investigations. Reconciling three-dimensional drop and seakeeping test results is at best difficult, so an experimental program was derived that would show comparison of the results of various techniques for the three hull forms given in Section 3.

As planned, the test program's main objectives were:

- to determine the form factor (or k-values) at each instrumented forward station;
- to compare the measured form factors with those predicted by the Ochi-Motter (OM) and the Stavovy-Chuang (SC) methods;
- to examine the effects of hull geometry on slam pressures;
- to develop a method for calculating the spatial and temporal variation of bow slam force.

The significant parameters measured during the experiments were the peak pressure value, rise time (from zero to maximum), duration of pressure pulse, the time between pulses, and the relative velocity between the hull and the water surface at the point of contact.

Three basic drop test configurations were selected, based on Schenzles' work<sup>8</sup>:

- even keel free drops in calm water,
- pivoted (rotational) drops in calm water, and
- pivoted (rotational) drops in regular waves;

as shown in Figure 15. Additionally, seakeeping experiments in regular head waves were included in the program.

### 5.1 Drop Test Programme

The drop tests were carried out in a 60 ft long basin with a plunger-type wave maker at one end and a sloping gravel beach on the other. A modified towing carriage capable of accommodating the drop test rig and achieving high forward speed was used for the tests. The basin had a 10 ft wide wave channel in its center with transparent walls at the test section.



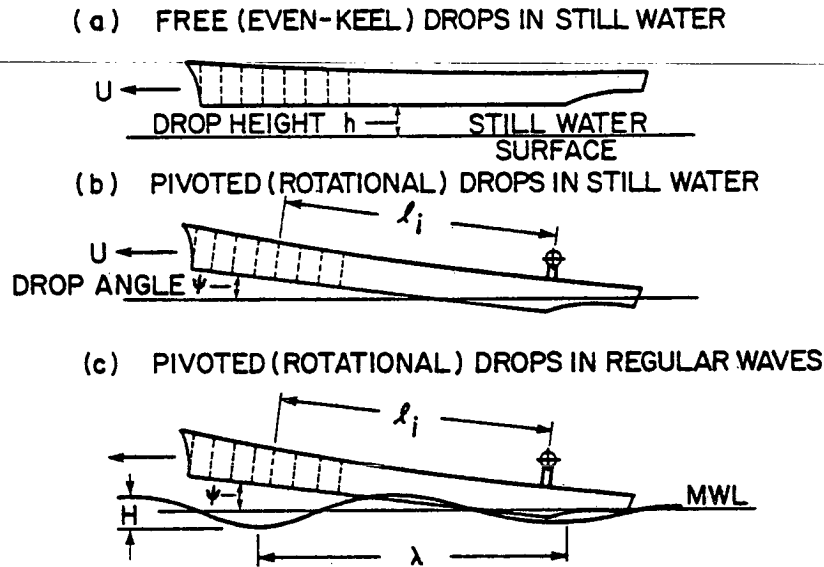


Figure 15 Drop Test Types

The three models shown in Figure 5 were fitted with twenty-six Kulite XTMS 1-190 series diaphragm-type pressure transducers effective in the range 0 to 50 psi. The gauges were installed along the keel on the centreline and on one side of the lower hull from the F.P. to station 7. Wherever possible three transducers were installed at positions less than 1/10 draft (0.1T) from the keel, where maximum pressures were expected. Above the 0.1T line, transducer locations were chosen to provide a reasonably accurate girthwise pressure profile, and a few were located near the load water line forward to measure flare slamming effects. The model was also fitted with a motions package consisting of accelerometers and attitude indicators.

The drop test program was designed to achieve a wide range of relative velocities within an acceptable time and cost. A total of 849 drop tests were performed with the three models. The vertical drop velocity was readily controlled by the drop height, which was restricted to a maximum of 12 inches to avoid complete submergence of the bow. For the same reason, the maximum initial trim angle in the pivoted tests was 14 degrees. Calm water drops were repeated three times. Drops in regular waves had no repeat runs due to the difficulty in repeatedly dropping the model at exactly the same position on the wave. Table I gives the ranges of the drop test variables.

TABLE I Ranges of Drop Test Variables

	<u>Minimum</u>	<u>Increment</u>	<u>Maximum</u>
Drop Heights	2"	2"	12"
Initial Trim Angles	2°	2°	14°
Approximate Forward Speeds	0	0.5m/s	3m/s

5.2 Seakeeping Test Programme

To complement the drop tests, ARCTEC conducted a limited number of seakeeping tests using the National Research Council (NRC) of Canada's facilities in Ottawa. Although the original plan included seakeeping experiments with all three models, experiments were carried out only with the V-form model due to data handling difficulties.

The model was self-propelled in regular head waves in NRC's ship model experiment tank, with the model-carriage connections allowing freedom in pitch, heave and surge only. The model was fitted with the same pressure transducer array as in the drop tests, together with accelerometers and sonic probes to derive motions. Relative motions were measured by means of capacitance probes on the model surface. The capacitance relative motion probes proved to be unsuitable for the derivation of instantaneous relative velocities. Without relative velocity at impact, form factors could not be derived accurately.

The seakeeping experiments were performed in three groups. In the first case, Froude number and wave frequency were varied to establish slamming zones, Table II. Then, wave slope was varied in the severe slamming region as shown in Table III. Finally, the bracketed experiment in Table II was repeated eleven times to obtain a measure of the scatter in the results.

The 89 test runs were expected to generate about 46 000 pressure peaks, calling for an unreasonable analysis effort. As a result, the analysis was restricted to seven transducers, using a PDP-11 computer digitising at 20 000 samples per second in the region of slams. Even with analysis of only 7 of 24 possible transducers, 50 hours of computer time were required for digitising.

TABLE II Slamming Zone Parameter Space in Seakeeping Tests

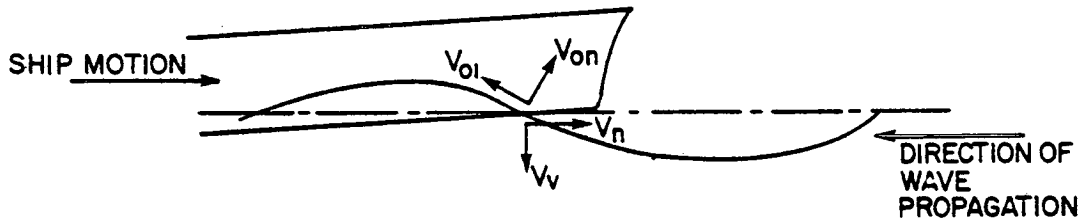
$\omega\sqrt{L/g}$	1.5	1.65	1.80	1.95	2.10	2.25	2.40	2.55	2.70	
$F_n$										
0.20										
0.25							X			
0.34					X	X	X			
0.35			X	X	X	X	X			
0.40			X	X	X	X	X			
0.45	X	X	X	X	X	X	X	X	X	
0.50	X	X	X	X	X	X	X			
0.55	X	X	X	X	(X)	X	X	X	X	
$100\zeta_A/\lambda$		1.18	1.23	0.99	1.04	1.22	1.33	1.56	1.60	1.55

severe  
slamming  
zone

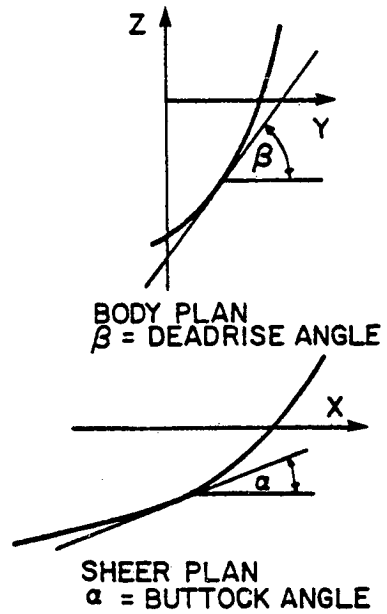
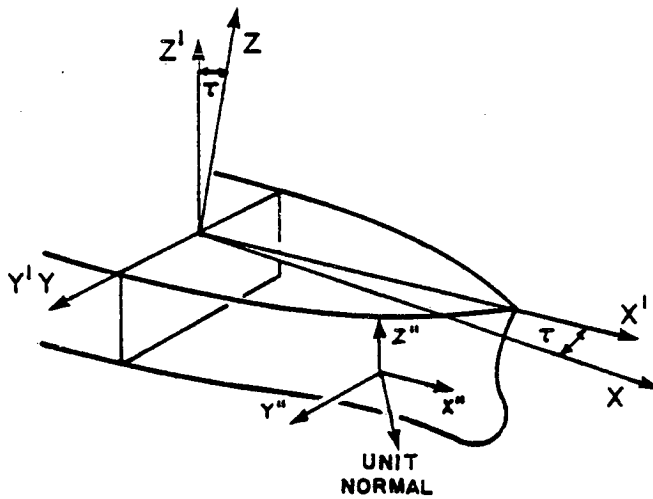
Table III Wave Slope Variation in Severe Slamming Zone

$\omega\sqrt{L/g}$	1.8	2.1	2.4
	$100\zeta_A/\lambda$ RANGE		
$F_n$			
0.35	0.99-2.05	1.20-1.94	1.48-2.32
0.45	0.99-2.00	1.23-1.88	1.53-2.48
0.55	0.93-1.47	1.22-1.77	1.56-2.29

(a) SHIP-WAVE VELOCITIES AT IMPACT



SHIP VELOCITIES  $V_n, V_v$   
 WATER VELOCITIES NORMAL & TANGENTIAL { WAVE SURFACE  $V_{on}, V_{oi}$   
 WAVE HEIGHT =  $H$  { HORIZONTAL, VERTICAL  $u, v$   
 WAVE LENGTH =  $\lambda$



(b) SHIP CO-ORDINATES AND ANGLES

Figure 16 Slam Geometry Definition

### 5.3 Results

#### 5.3.1 Drop Tests

For the drop tests, the clear-walled wave channel allowed use of a video camera to record impacts, so that impact velocity and form factor could be reliably determined. The keel slam pressure is defined as follows,

$$p = (\rho/2)k'V^2 \tag{12}$$

$$k' = k/(1 + \tan \beta \cos^2 \alpha) \tag{13}$$

$$V = V_h (V_{ot} \cos \theta + V_{on} \sin \theta) \sin (\alpha + \tau) + V_v (V_{on} \cos \theta - V_{ot} \sin \theta) \cos (\alpha - \tau) \tag{14}$$

where the angles are defined in Figure 16 and the nomenclature.

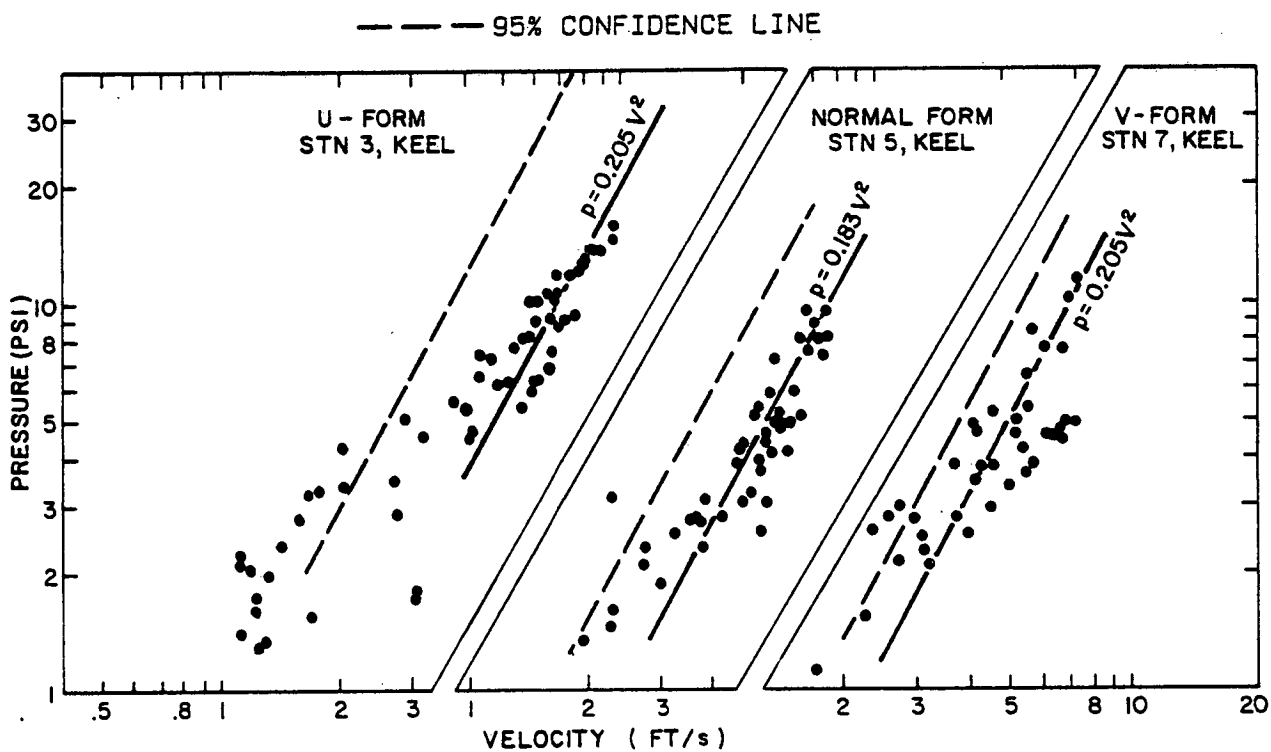


Figure 17 Typical Pressure Plots from Stillwater Pivoted Drops

Typical results of the drop tests are shown in Figure 17 as pressure-velocity plots, together with derived dimensional form factors. It was apparent that 2 is not necessarily the most suitable index of velocity for predicting pressure, but this value was used in the conventional manner. In reality the index varied from 1.5 to 2.5, but this variation may be safely ignored considering that 95 percent confidence limits for the derived coefficients encompass most of the data. Indeed, for design use, the upper 95th percentile limits, shown in Figure 17, could be considered more suitable predictors than the mean lines, although the mean value is appropriate for use of equation (10) for the prediction of design pressures.

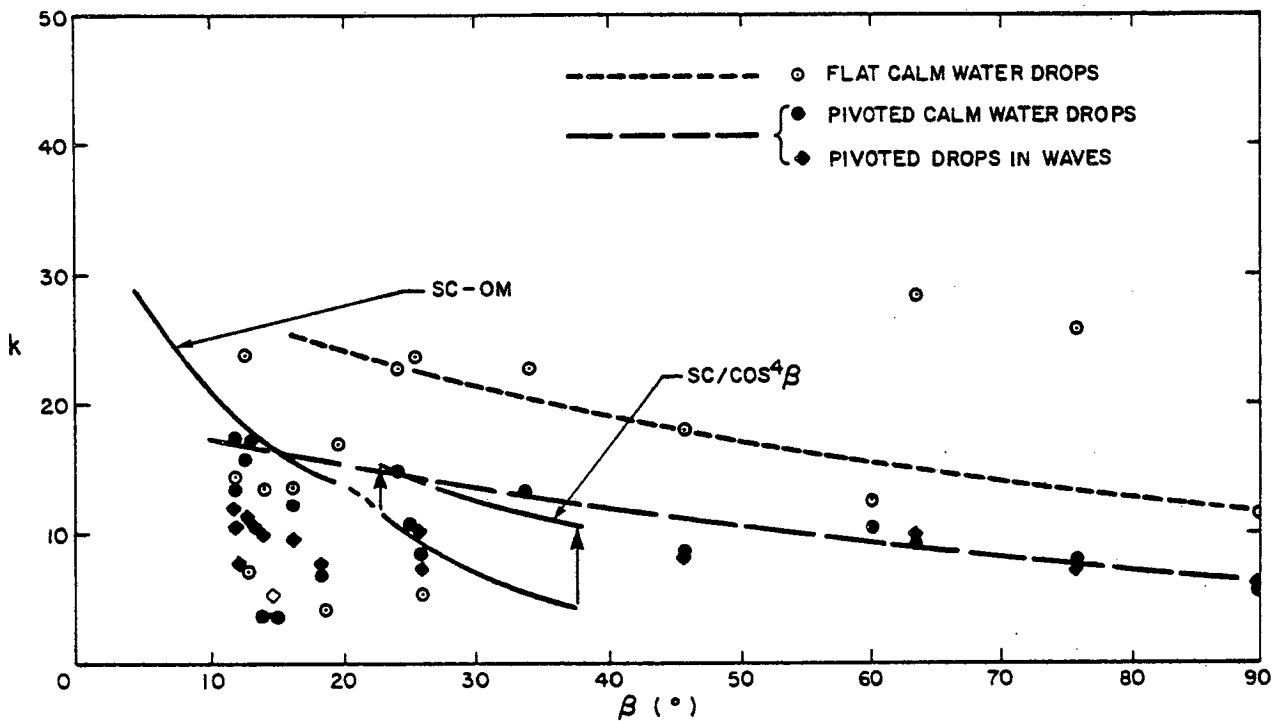


Figure 18 Experimental Drop Test Form Factors for Keel

Figure 18 shows a comparison of form factors derived from the drop tests, together with the SC-OM line first shown in Figure 3. As anticipated, there are differences between the flat and pivoted drop form factors, the former giving clearly larger pressures, except at low deadrise angles. The heavy scatter and reduced pressures seen at deadrise angles below 30 degrees could be due to air entrapment, but it is hard to credit this at deadrise angles above five degrees. The pivoted drop results run into the upper, Ochi-Motter, portion of the SC-OM line in Figure 18, but lie nearly an order of magnitude higher than the lower, Stavovy-Chuang portion. A plausible explanation for this disconcerting behaviour is available.

Schmitke<sup>9</sup> produced the composite SC-OM line by joining the two predictions where they crossed. Unfortunately, whereas Ochi-Motter predict  $k$ , Stavovy-Chuang predict  $k_1^{11,17}$ , where

$$k = k_1 / \cos^4 \beta \quad (15)$$

The chain-dotted line in Figure 18 shows that correction of the lower portion of the SC-OM by the  $\cos^4 \beta$  divisor would improve agreement considerably.

Figure 18 also shows that keel form factor results for normal, U- and V-form models collapse to a single line when plotted to a base of  $\beta$ , implying that hull form, per se, is not so important as deadrise angle. This is the conventional assumption.

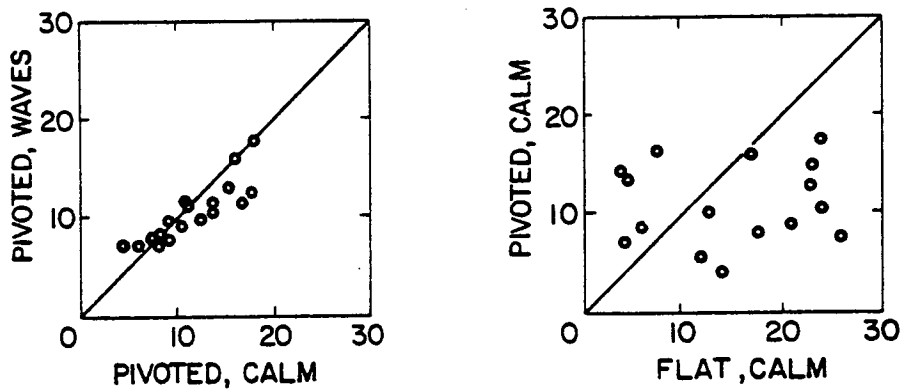
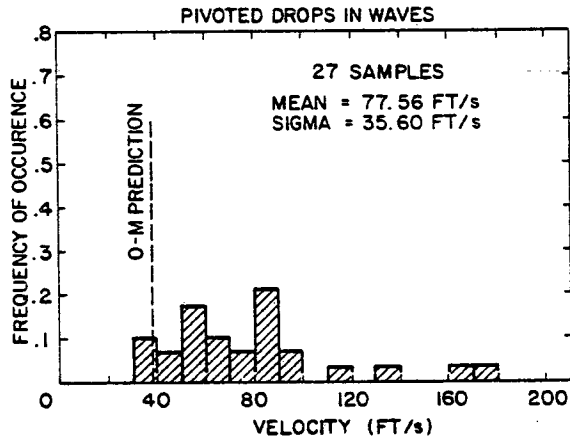


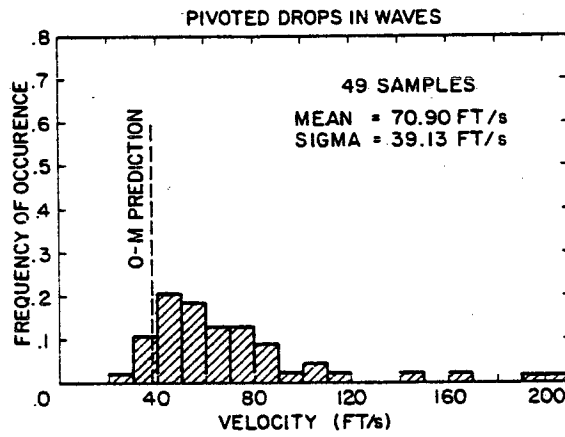
Figure 19 Comparison of Form Factor from Different Drop Test Types

Figure 19 compares derived form factors at individual stations to indicate differences between test techniques. Even in the reduced pressure zone (see Figure 18,  $\beta < 25^\circ$ ) pivoted drops in waves and in calm water yield consistent form factors. Conversely, comparison of the pivoted calm and flat calm results does not even suggest a relationship between the results of the two techniques. Perhaps this should be an expected result given the level of scatter in the flat calm line (Figure 18) at all deadrise angles. The value of flat drops in calm water must be questioned.

Velocity of Pressure Pulse Along Keel Model No. 266 (Extreme U)



Model No. 264 (Normal)



Model No. 267 (Extreme V)

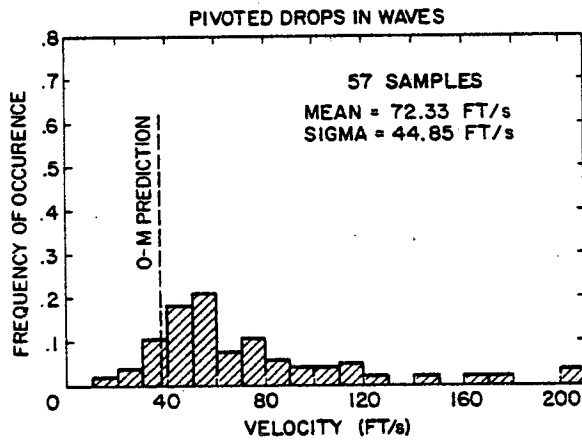
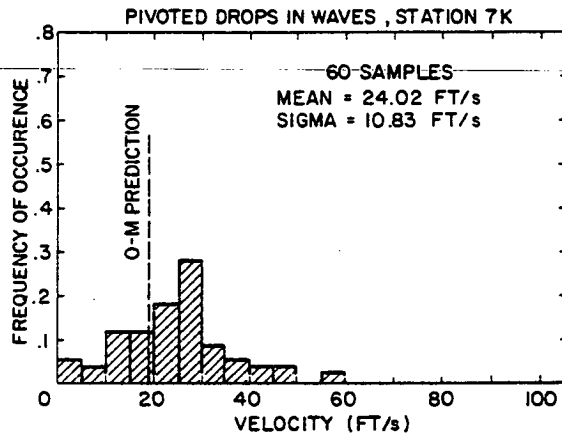


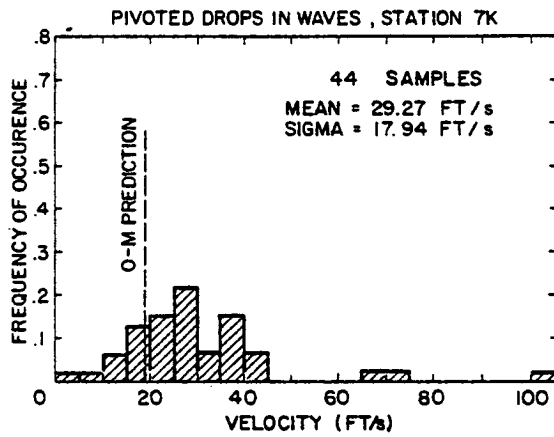
Figure 20 Slam Pressure Pulse Velocities



Velocity of Pressure Pulse Along Girth Model No. 266 (Extreme U)



Model No. 264 (Normal)



Model No. 267 (Extreme V)

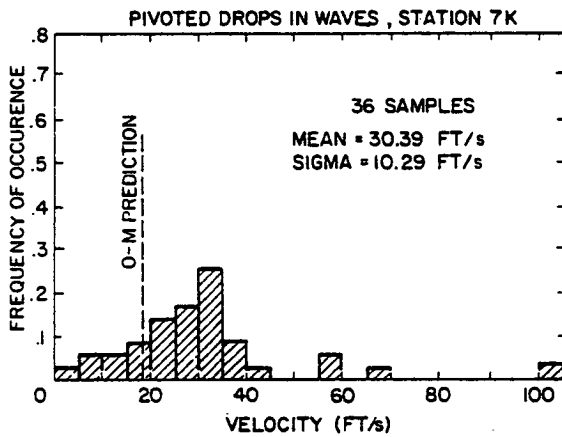


Figure 20 Slam Pressure Pulse Velocities cont'd

Figure 20 shows histograms of slam pressure pulse velocity along both the keel and the girth for pivoted drops in waves. The average pressure pulse velocity is consistently higher than predicted by Ochi and Motter.

### 5.3.2 Seakeeping Tests

Failure of the seakeeping model relative motion gauges prevented the derivation of instantaneous relative velocities at impact, so it was necessary to use pitch and heave amplitudes and their average phases relative to the waves to estimate impact velocities. This was the source of considerable scatter in pressure velocity plots, so form factors were not derived; however, the seakeeping data should not be discounted.

It is revealing to superimpose seakeeping and pivoted drop results, as in Figure 21, for consistency of the two methods is clear; however, there is a disturbing amount of scatter at low pressures. There is also a suggestion that a common envelope encloses the two results; if so, the seakeeping tests might have benefitted from more extreme waveheight, notwithstanding difficulties with relative velocity measurement. More important, a statistical estimate of the upper envelope is potentially as useful a measure of pressure as the mean line used conventionally.

Figure 22 shows the poor repeatability of peak slamming pressures, with near order of magnitude variations. The variations, probably due to the typical characteristics of NRC's pneumatic wavemaker, would not be of importance had relative velocity been measured, but the absence of such measurements prevents the derivation of reliable form factors.

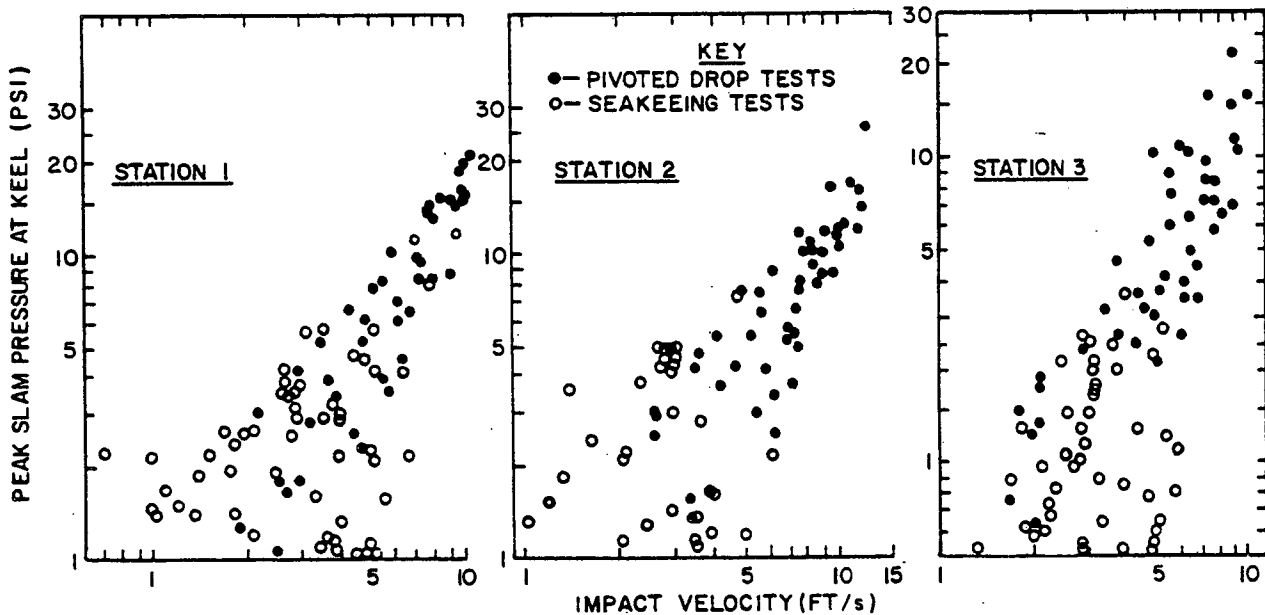


Figure 21 V-Form Model Pressure-Velocity Relationships:  
Comparison of Pivoted Drop and Seakeeping Tests

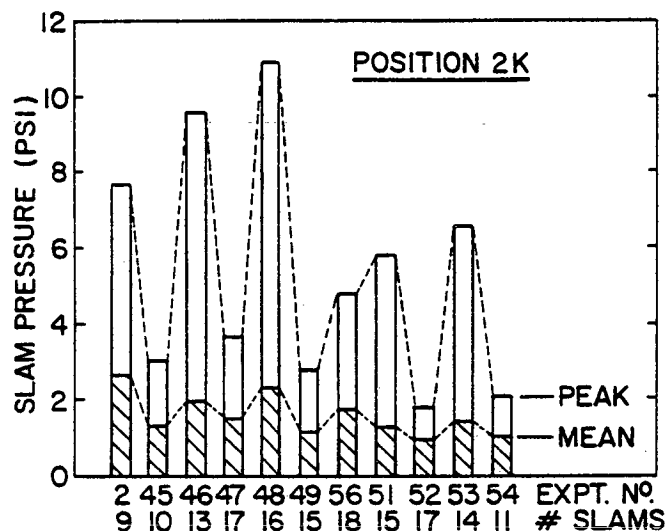


Figure 22 Repeatability of Slam Pressures During Seakeeping Tests

#### 6. SIMULATION/MODEL TEST COMPARISONS

Direct comparison between simulation and model test results is precluded by the noise content of the simulations and by different impact dynamics in each case. Nonetheless, this section highlights qualitative similarities observed in the development of the pressure signature around the girth.

A typical set of model test pressure traces is sketched in Figure 23. These data are at station 5 for a pivoted drop in calm water with an initial full scale impact velocity of approximately 20 fps. Pressures were recorded on the keel and at three locations A, B and C towards the waterline as shown in Figure 5. Different levels of ambient noise on each trace reflect different calibrations for each transducer.

The features seen in this figure are typical. The large oscillations on the keel trace may be due to air entrapment. At locations close to the keel, A and B, the pressure rise is almost instantaneous; at location C it is generally one to several orders of magnitude slower, depending upon the initial impact velocity. It is not possible, given the spatial resolution of these pressure measurements, to determine whether this pressure rise character change is gradual or abrupt. Also note that the initial peak remains reasonably constant between the keel and B, but is significantly reduced at C.

The dynamics of impact are different between a pivoted three-dimensional drop and a simulated two-dimensional drop. Most notably, the times at which off-keel peaks are recorded in the example shown in Figure 23 suggest that the model is still accelerating after initial impact, whereas the equivalent two-dimensional simulation demonstrates a small deceleration almost immediately.

Despite the above, and ignoring the keel oscillations, the pressure traces in Figure 23 are consistent with the observations in Section 4.6 that the girthwise pressure distribution is initially Wagner-like, that is, peaked at the waterline, (at least to B). Further around the girth, the pressure pulse becomes much more spread out resulting in a more uniform pressure distribution, tending to triangular as the pulse disappears altogether. In Figure 24, data from drop 438 are plotted with data from the corresponding simulation. The development of the pressure distribution as described above can be seen in both cases.

The transition from a Wagner to a triangular pressure distribution occurs as local deadrise is increasing, and may be associated with a critical value of deadrise. The simulations suggest that this transition is fairly abrupt in time, as shown in Figure 24 between step 72 and step 84. The value of deadrise for this transition, estimated from the simulation data, is shown in Figure 25. There is no systematic variation of transition position with impact velocity.

The width of the transition region in Figure 25 is due to numerical scatter in the simulations. Since the critical deadrise angle for transition differs for each station in Figure 25, transition is not a function of deadrise angle alone, unlike form factor. In addition, extrapolation suggests that for fuller sections, the critical value of deadrise may be quite low.

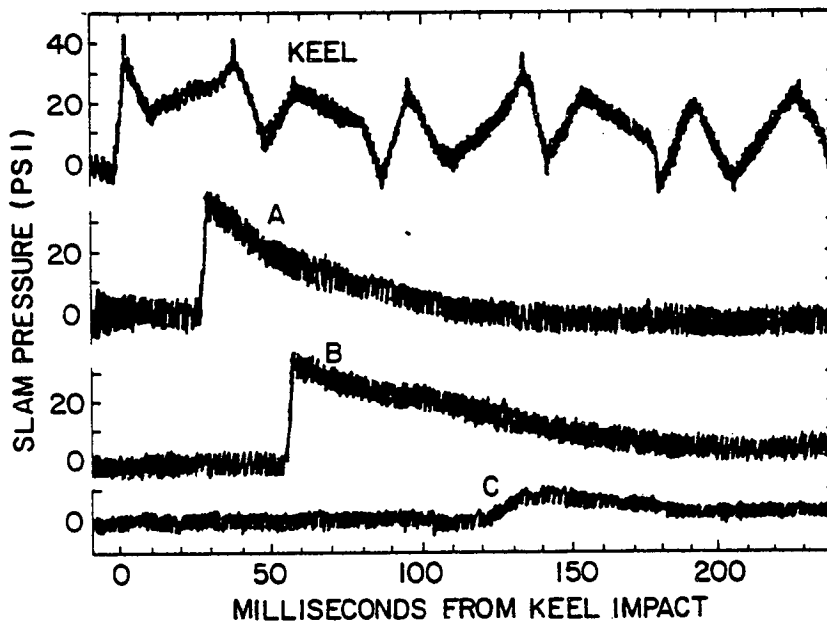


Figure 23 Drop 438, Sketch of Pressure Signatures at Station 5, to full scale

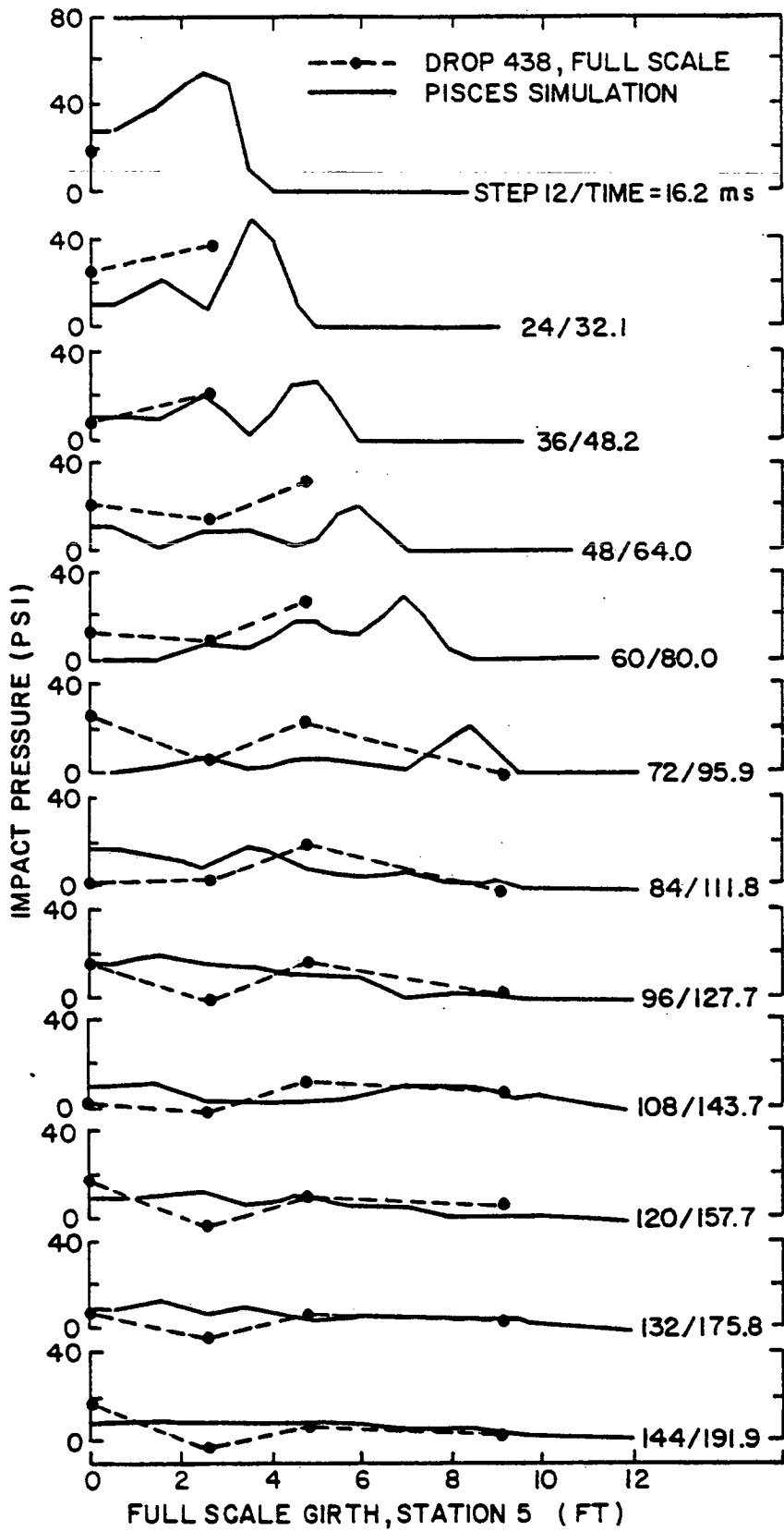


Figure 24 Comparison of Pressure Distribution Development

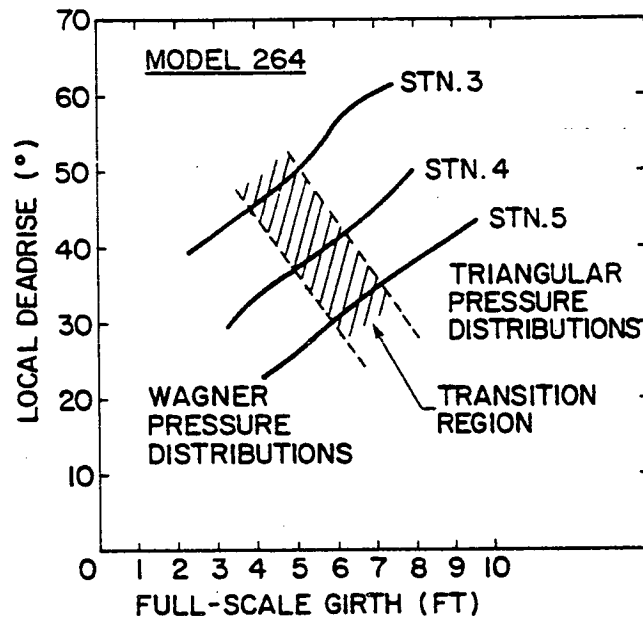


Figure 25 Transition from Wagner to Triangular Girthwise Pressure Distribution from Simulation Data

7. CONCLUDING REMARKS

The work described in this memorandum has been aimed towards the eventual development of accurate slamming prediction capabilities for warship hulls. The initial tasks, presented here, consist of a comprehensive set of model experiments, undertaken by ARCTEC Canada Ltd., to provide a database of slamming data; and a series of numerical simulations to provide further insight into the fundamental processes of slamming and to aid with interpretation of the data. The simulations were restricted by computational complexity to two dimensions.

Results from the numerical simulations agree well with two-dimensional theories and drop test data. The surge ratio,  $\mu$ , plays a significant role in two dimensional drop dynamics, although it is not clear to what extent this translates into three dimensions. Numerical noise made it necessary to smooth the results and made peak pressure determination uncertain.

A notable aspect of the simulation results was the transition of the developing bottom pressure distribution from a classic, Wagner, form to a uniform, or triangular, shape. This transition appears to be fairly abrupt, and may be associated with quite low local deadrise angles for full sections, although it is clearly not a function of deadrise alone.

The transition was also noted on the higher deadrise angle wedge simulations, but was much delayed. Although spatial resolution of the bottom pressure was low, the experimental data appears to confirm the existence of this phenomenon for three dimensional hulls.

In the experimental program, the results from the extensive drop test series and the more limited seakeeping experiments demonstrated that pivoted drop testing is a useful model experimental technique from which the slamming characteristics of warship hull forms can be evaluated. A good consistency was found between pivoted drops, both in calm water and in waves, and seakeeping tests.

The experimental results show a fair degree of scatter, particularly at low impact velocities. These uncertainties are primarily in the measurement of impact velocity, which needs further attention in future work. Nonetheless, predictions of pressure-velocity relationships and the derived form factors are satisfactory for design applications.

A notable departure from previous theories is that the slam pressure pulse velocities observed for pivoted drops in waves were consistently higher than predicted by Ochi and Motter. Also, the previously adopted Stavovy Chuang-Ochi Motter line appears to underpredict form factors at deadrise angles greater than 25 degrees, apparently due to misinterpretation of the original Stavovy-Chuang data.

Consideration of the progress achieved this far leads to the following recommendations for further investigation:

- An improved technique for impact velocity measurement is required, possibly using some form of emergence probe.
- Specific experiments and numerical simulations should be conducted to clarify further some of the fundamental features of slamming, such as the spatial distribution and time history of pressures, particularly in three dimensions.
- A larger experimental database is required to allow the establishment of reliable empirical prediction methods.

## 8. ACKNOWLEDGEMENTS

The foundations of this research program were laid by Mr. R.T. Schmitke, formerly Leader, Ship Dynamics Group, DREA, now Head, Military Engineering Section, Defence Research Establishment Suffield. Mr. J.R. Gandier of CDC CYBERNET Services, Ottawa, performed the PISCES computer simulations.

## REFERENCES

1. Mackay, M. and Schmitke, R.T.: 'PHHS, A FORTRAN Programme for Ship Pitch, Heave and Seakeeping Prediction', DREA Technical Memorandum 78/B, April 1978.
2. Salvensen, N., Tuck, E.O., and Faltinsen, O.: 'Ship Motions and Sea Loads', Trans. SNAME, Vol 78, 1970.
3. Schmitke, R.T.: 'Ship Sway, Roll and Yaw Motions in Oblique Seas', Trans. SNAME, Vol. 86, 1978.
4. Andrew, R.N. and Lloyd, A.R.J.M.: 'Full-Scale Comparative Measurements of the Behaviour of Two Frigates in Severe Head Seas', Trans. RINA, Vol 123, 1981.
5. Ochi, M.K. and Motter, L.E.: 'Prediction of Slamming Characteristics and Hull Responses for Ship Design', Trans. SNAME, Vol. 81, 1973.
6. Chuang, S.L.: 'Slamming Tests of Three-Dimensional Models in Calm Water and Waves', NSRDC Report 4095, September 1973.
7. Ochi, M.K. and Bonilla-Norat, J.: 'Pressure-Velocity Relationship in Impact of a Ship Model Dropped onto the Water Surface and in Slamming in Waves', Naval Ship Research and Development Center Report 3153, 1970.
8. Schenzle, P., Broelmann, J., and Blume, P.: 'Systematische Untersuchung von Slamming - Drücken mit Hilfe von Dreh-Fall-Versuchen in Wellen', Institut für Schiffbau, Universität of Hamburg, Bericht Nr. 270, 1971.
9. Schmitke, R.T.: 'Improved Slamming Predictions for the PHHS Computer Program', DREA Technical Memorandum 79/A, February 1979.
10. Ochi, M.K. and Motter, L.E.: 'A Method to Estimate Slamming Characteristics for Ship Design', Marine Technology, April 1971.
11. Stavovy, A.B. and Chuang, S.L.: 'Analytical Determination of Slamming Pressures for High-Speed Vehicles in Waves", J. Ship Research, Vol. 20, December 1976.
12. Schmitke, R.T. and Murdey, D.C.: 'Seakeeping and Resistance Trade-Offs in Frigate Hull Form Design', Proc. Thirteenth ONR, Tokyo, 1980.

PRECEDING PAGE BLANK



13. Hancock, S.L.: 'Finite Difference Equations for PISCES 2DELK, A Coupled Euler Lagrange Continuum Mechanics Computer Program', Physics International Company Technical Memo TCAM 76-2, April 1976.
14. Geers, T.L., Loden, W.A. and Yee, H.C.: 'Boundary-Element Analysis of Fluid-Solid Impact', Winter Annual Meeting of the American Society of Mechanical Engineers, 1977, AMD-Vol. 26.
15. Chu, W.H. and Abramson, H.N.: 'Hydrodynamic Theories of Ship Slamming - Review and Extension', Journal of Ship Research, Vol. 4, No. 4, March 1961.
16. Wagner, H.: 'Über-Stoss- und Gleitvorgänge an der Oberfläche von Flüssigkeiten', Zeitschrift für angewandte Mathematik und Mechanik, Vol. 12 No. 4, Berlin, August 1932.
17. Graham, R.: Private communication.

# UNLIMITED DISTRIBUTION

UNCLASSIFIED

Security Classification

DOCUMENT CONTROL DATA - R & D		
(Security classification of title, body of abstract and indexing annotation must be entered when the overall document is classified)		
1. ORIGINATING ACTIVITY	2a. DOCUMENT SECURITY CLASSIFICATION <b>UNCLASSIFIED</b>	
	2b. GROUP	
3. DOCUMENT TITLE  <b>Some Warship Slamming Investigations</b>		
4. DESCRIPTIVE NOTES (Type of report and inclusive dates)  <b>Technical Memorandum</b>		
5. AUTHOR(S) (Last name, first name, middle initial)  <b>Nethercote, W.C.E., Mackay, M, Menon, B.</b>		
6. DOCUMENT DATE <b>January 1986</b>	7a. TOTAL NO. OF PAGES <b>41</b>	7b. NO. OF REFS <b>17</b>
8a. PROJECT OR GRANT NO.	9a. ORIGINATOR'S DOCUMENT NUMBER(S)  <b>DREA TECHNICAL MEMORANDUM 86/206</b>	
8b. CONTRACT NO.	9b. OTHER DOCUMENT NO.(S) (Any other numbers that may be assigned this document)	
10. DISTRIBUTION STATEMENT  <b>Unlimited</b>		
11. SUPPLEMENTARY NOTES	12. SPONSORING ACTIVITY	
13. ABSTRACT  Excessive slamming is the most common cause of speed reduction for frigates and destroyers in heavy head seas. DREA's early interest in frigate/destroyer slamming was limited to the development of computer programs for ship seakeeping performance prediction. Published bottom slamming algorithms were adopted and refined to provide a slamming prediction capability for DREA software. In follow-on work described herein, both two-dimensional numerical simulations and three-dimensional model tests were performed by contractors to obtain better physical insight and expand the empirical data base. The two-dimensional numerical simulation results required considerable smoothing to reduce numerical noise, but still yielded form factors in satisfactory agreement with two-dimensional theoretical and experimental results. The simulations also gave unique insight into the girthwise development of slamming pressures. The three-dimensional model tests indicated that pivoted drop tests in waves may be substituted for conventional seakeeping tests, but the general applicability of the results was limited by difficulties with measurement of relative impact velocity. Notwithstanding the velocity measurement difficulties, the three-dimensional tests provided important information on longitudinal and girthwise pressure pulse velocities. Further experimental work will be required to develop a usable experimental data base.		

## KEY WORDS

warship  
 frigate  
 destroyer  
 bottom slamming  
 seakeeping

## INSTRUCTIONS

1. **ORIGINATING ACTIVITY:** Enter the name and address of the organization issuing the document.
- 2a. **DOCUMENT SECURITY CLASSIFICATION:** Enter the overall security classification of the document including special warning terms whenever applicable.
- 2b. **GROUP:** Enter security reclassification group number. The three groups are defined in Appendix 'M' of the DRB Security Regulations.
3. **DOCUMENT TITLE:** Enter the complete document title in all capital letters. Titles in all cases should be unclassified. If a sufficiently descriptive title cannot be selected without classification, show title classification with the usual one-capital-letter abbreviation in parentheses immediately following the title.
4. **DESCRIPTIVE NOTES:** Enter the category of document, e.g. technical report, technical note or technical letter. If appropriate, enter the type of document, e.g. interim, progress, summary, annual or final. Give the inclusive dates when a specific reporting period is covered.
5. **AUTHOR(S):** Enter the name(s) of author(s) as shown on or in the document. Enter last name, first name, middle initial. If military, show rank. The name of the principal author is an absolute minimum requirement.
6. **DOCUMENT DATE:** Enter the date (month, year) of Establishment approval for publication of the document.
- 7a. **TOTAL NUMBER OF PAGES:** The total page count should follow normal pagination procedures, i.e., enter the number of pages containing information.
- 7b. **NUMBER OF REFERENCES:** Enter the total number of references cited in the document.
- 8a. **PROJECT OR GRANT NUMBER:** If appropriate, enter the applicable research and development project or grant number under which the document was written.
- 8b. **CONTRACT NUMBER:** If appropriate, enter the applicable number under which the document was written.
- 9a. **ORIGINATOR'S DOCUMENT NUMBER(S):** Enter the official document number by which the document will be identified and controlled by the originating activity. This number must be unique to this document.
- 9b. **OTHER DOCUMENT NUMBER(S):** If the document has been assigned any other document numbers (either by the originator or by the sponsor), also enter this number(s).
10. **DISTRIBUTION STATEMENT:** Enter any limitations on further dissemination of the document, other than those imposed by security classification, using standard statements such as:
  - (1) "Qualified requesters may obtain copies of this document from their defence documentation center."
  - (2) "Announcement and dissemination of this document is not authorized without prior approval from originating activity."
11. **SUPPLEMENTARY NOTES:** Use for additional explanatory notes.
12. **SPONSORING ACTIVITY:** Enter the name of the departmental project office or laboratory sponsoring the research and development. Include address.
13. **ABSTRACT:** Enter an abstract giving a brief and factual summary of the document, even though it may also appear elsewhere in the body of the document itself. It is highly desirable that the abstract of classified documents be unclassified. Each paragraph of the abstract shall end with an indication of the security classification of the information in the paragraph (unless the document itself is unclassified) represented as (TS), (S), (C), (R), or (U).  
  
The length of the abstract should be limited to 20 single-spaced standard typewritten lines; 7 1/4 inches long.
14. **KEY WORDS:** Key words are technically meaningful terms or short phrases that characterize a document and could be helpful in cataloging the document. Key words should be selected so that no security classification is required. Identifiers, such as equipment model designation, trade name, military project code name, geographic location, may be used as key words but will be followed by an indication of technical context.